

# SI Appendix: Mutations associated with familial Parkinson's disease alter the initiation and amplification steps of $\alpha$ -synuclein aggregation

Patrick Flagmeier<sup>a</sup>, Georg Meisl<sup>a</sup>, Michele Vendruscolo<sup>a</sup>, Tuomas P.J. Knowles<sup>a</sup>, Christopher M. Dobson<sup>a,1</sup>, Alexander K. Buell<sup>a,b,1</sup>, and Céline Galvagnion<sup>a,1</sup>

<sup>a</sup>Department of Chemistry, University of Cambridge, Lensfield Road, Cambridge CB2 1EW, UK; <sup>b</sup>Present address: Institute of Physical Biology, University of Düsseldorf, Universitätsstr.1, 40225 Düsseldorf, Germany; <sup>1</sup>To whom correspondence should be addressed. E-mail: cmd44@cam.ac.uk, Alexander.Buell@uni-duesseldorf.de, cg393@cam.ac.uk

## 1. SI Methods

**Reagents.** Thioflavin T UltraPure Grade (ThT > 95%) was purchased from Eurogentec Ltd (Belgium). Sodium phosphate monobasic (NaH<sub>2</sub>PO<sub>4</sub>, BioPerformance Certified > 99.0%), sodium phosphate dibasic (Na<sub>2</sub>HPO<sub>4</sub>, ReagentPlus, > 99.0%) and sodium azide (NaN<sub>3</sub>, ReagentPlus, > 99.5%) were purchased from Sigma Aldrich, UK. 1,2-Dimyristoyl-sn-glycero-3-phospho-L-serine, sodium salt (DMPS) was purchased from Avanti Polar Lipids, Inc, USA.

**Protein preparation.**  $\alpha$ -synuclein variants were expressed and purified as described previously [1–3]. To determine the concentrations in solution we used the absorbance value of the protein measured at 275 nm and an extinction coefficient of 5,600 M<sup>-1</sup>. The protein solutions were divided into aliquots, flash frozen in liquid N<sub>2</sub> and stored at -80°C, until required for use.

**Seed fibril formation.** Seed fibrils were produced as described previously [1]. 500  $\mu$ L samples of  $\alpha$ -synuclein at concentrations from 500–800  $\mu$ M were incubated in 20 mM phosphate buffer (pH 6.5) for 48–72 h at ca. 40°C and stirred at 1,500 rpm with a Teflon bar on an RCT Basic Heat Plate (IKA, Staufen, Germany). Fibrils were diluted to a monomer equivalent concentration of 200  $\mu$ M, divided into aliquots, flash frozen in liquid N<sub>2</sub> and stored at -80°C. For experiments at pH 6.5 and  $\mu$ M fibril concentrations the 200  $\mu$ M fibril stock was sonicated for between 0.5 and 1 min using a probe sonicator (Bandelin, Sonopuls HD 2070, Berlin, Germany), using 10% maximum power and a 50% cycle. For experiments at low pH with nM fibril concentrations the 200  $\mu$ M stock was diluted to 10  $\mu$ M in water, sonicated 3 times for 5 s using 10% maximum power and 50% cycles using the probe sonicator.

**Lipid vesicle preparation.** DMPS lipid powder was dissolved in 20 mM phosphate buffer (NaH<sub>2</sub>PO<sub>4</sub>/Na<sub>2</sub>HPO<sub>4</sub>), pH 6.5, 0.01% NaN<sub>3</sub> and stirred at 45°C for at least 2 h. The solutions were then frozen and thawed five times using dry ice and a water bath at 45°C. Lipid vesicles were prepared by sonication (Bandelin, Sonopuls HD 2070, 3 x 5 min, 50% cycle, 10% maximum power) and centrifuged at 15,000 rpm for 30 min at 25°C. The average size of the vesicles was checked by

dynamic light scattering (Zetasizer Nano ZSP, Malvern Instruments, Malvern, UK) to ensure a distribution centered at a diameter of 20 nm.

**AFM images and analysis.** Atomic force microscopy images were taken using a Nanowizard II atomic force microscope (JPK, Berlin, Germany) using tapping mode in air. Solutions containing fibrils were diluted to a monomer concentration of 1  $\mu\text{M}$  in water and 10  $\mu\text{L}$  samples of the diluted solution were deposited on freshly cleaved mica and left to dry for at least 30 min. The samples were carefully washed with 50  $\mu\text{L}$  of water and then dried again. The images were loaded into the freely available software Gwyddion and the profile function was used to extract a height profile. To determine the fibril thickness the baseline height of the image was subtracted from the fibril height.

**CD spectroscopy.** CD samples were prepared by incubating 20  $\mu\text{M}$  WT  $\alpha$ -synuclein or each of the different variants in the presence of increasing concentrations of DMPS in 20 mM phosphate buffer, pH 6.5. Far-UV CD spectra were recorded on a JASCO J-810 spectrophotometer (JASCO UK, Ltd) equipped with a Peltier thermally controlled cuvette holder at 30°C. Quartz cuvettes with path lengths of 1 mm were used and CD spectra were obtained by averaging five individual spectra recorded between wavelengths of 250 and 200 nm, with a bandwidth of 1 nm, a data pitch of 0.2 nm, a scanning speed of 50 nm/min, and a response time of 1 s. Each value of the CD signal intensity reported at 222 nm corresponds to the average of 60 measurements. For each protein sample, the CD signal of the buffer used to solubilize the protein was recorded and subtracted from the CD signal of the protein. The CD data were analyzed as previously described [2]. In brief, the observed CD signal ( $CD_{obs}$ ) consists of the sum of the signals of the lipid-bound and free  $\alpha$ -synuclein:

$$CD_{obs} = x_{\alpha-syn_B} CD_B + x_{\alpha-syn_F} CD_F \quad [1]$$

where  $x_{\alpha-syn_B}$  and  $x_{\alpha-syn_F}$  are the fractions of  $\alpha$ -synuclein bound to the membrane and free in solution, respectively, and  $CD_B$  and  $CD_F$  are the CD signals of the bound and free forms of  $\alpha$ -synuclein, respectively. By assuming that  $x_{\alpha-syn_B} + x_{\alpha-syn_F} = 1$ , and that the signals of  $\alpha$ -synuclein in the presence of buffer, or in the presence of model membranes under saturating conditions, correspond to  $CD_F$  and  $CD_B$ , respectively, the fraction of  $\alpha$ -synuclein bound to SUV for each sample can be expressed as:

$$x_{\alpha-syn_B} = \frac{CD_{obs} - CD_F}{CD_B - CD_F} \quad [2]$$

We used the following model:  $\alpha - syn + lipid_L \rightleftharpoons \alpha - syn(lipid)_L$ , which corresponds to a non-cooperative binding Langmuir-Hill adsorption model, and the following equation to fit the measured CD signal:

$$x_{\alpha-syn_B} = \frac{([\alpha - syn] + \frac{[lipid]}{L} + K_D) - \sqrt{([\alpha - syn] + \frac{[lipid]}{L} + K_D)^2 - \frac{4[lipid][\alpha - syn]}{L}}}{2[\alpha - syn]} \quad [3]$$

where  $K_D$  (in M) is the dissociation constant and  $L$  is the number of lipid molecules interacting with one molecule of  $\alpha$ -synuclein.

**Differential scanning calorimetry.** DSC thermograms were acquired using a Microcal VP-DSC calorimeter (Malvern Instruments, Malvern, UK) with a scanning rate of  $1^{\circ}\text{C}\cdot\text{min}^{-1}$ . Protein and lipid samples were degassed for 20 min at room temperature prior to the measurements. For each sample, the DSC thermogram of the buffer was subtracted from that of the sample.

**Measurement of aggregation kinetics.** WT  $\alpha$ -synuclein or its variants were incubated at the concentrations indicated and in the presence of  $50\ \mu\text{M}$  ThT and either preformed fibrils or DMPS vesicles at  $37^{\circ}\text{C}$  or  $30^{\circ}\text{C}$ , respectively [1, 2]. The change in the ThT fluorescence signal was monitored using a Fluostar Optima or Polarstar Omega fluorescence plate reader (BMG Labtech, Aylesbury, UK) in bottom reading mode under quiescent conditions. Corning 96 well plates with half-area (3881, polystyrene, black with clear bottom) non-binding surfaces sealed with metal sealing tape were used for each experiment. For experiments involving shaking (orbital shaking for 300 s at 1,100 rpm), glass beads were introduced in the wells of the plate prior to the measurement and the change in the ThT fluorescence signal was monitored using a Polarstar Omega fluorescence plate reader. At the end of each aggregation experiment the concentrations of monomeric and fibrillar states of the protein were determined as described previously [2].

## 2. SI Analysis of the aggregation kinetics

### Determination of the lipid-induced aggregation rate.

**Kinetic analysis of the early time points of the aggregation curves of WT  $\alpha$ -synuclein and of the A30P, E46K, H50Q, A53T variants.** The change in mass concentration of fibrils with time  $M(t)$  was fitted [4] using the model described previously [2] and the following equation:

$$M(t) = \frac{K_M k_+ m(0)^{n+1} k_n b t^2}{2(K_M + m(0))} \quad [4]$$

where  $k_+$  is the elongation rate constant of fibrils from lipid vesicles,  $k_n$  is the heterogeneous primary nucleation rate constant,  $n$  is the reaction order of the heterogeneous primary nucleation reaction relative to the free monomer,  $m$ ,  $b$  is the total mass concentration of the protein bound to the lipid at 100% coverage ( $b = \frac{[\text{DMPS}]}{L}$ , with  $L$  the stoichiometry) and  $K_M$  is the Michaelis constant (fixed at 125  $\mu\text{M}$  for each mutant, as determined previously [2]). This global analysis yields  $k_n k_+$  and  $n$ , for each variant. We then estimated the rate of aggregation of each variant on lipid vesicles,  $\left(\frac{dM(t)}{dt}\right)_{\text{variant}} = \frac{K_M k_+ k_n \text{variant} b m_{\text{variant}}(0)^{n, \text{variant}} t}{4(K_M + m_{\text{variant}}(0))}$ , relative to that of the WT protein, for the same initial concentrations of free monomer and monomer bound to the lipid, i.e.  $m_{\text{variant}}(0) = m_{\text{WT}}(0)$  and  $b_{\text{variant}} = b_{\text{WT}}$ , respectively, using the following equation:

$$\text{Relative rate of aggregation on vesicles} = \frac{\left(\frac{dM(t)}{dt}\right)_{\text{variant}}}{\left(\frac{dM(t)}{dt}\right)_{\text{WT}}} = \frac{(k_n k_+)_{\text{variant}} m(0)^{n, \text{variant}}}{(k_n k_+)_{\text{WT}} m(0)^{n, \text{WT}}} \quad [5]$$

### Determination of the upper bound of the relative rate of lipid-induced aggregation of G51D $\alpha$ -synuclein.

Our data suggest that the G51D variant does not form detectable fibrils even when the protein is incubated for 65 h in the presence of 100  $\mu\text{M}$  DMPS. We have shown previously that the upper bound of the concentration of fibrils that can be detected using our ThT assay is 0.4  $\mu\text{M}$  [2]. We therefore estimated the upper limit of  $\left(\frac{dM(t)}{dt}\right)_{\text{G51D}} = \frac{K_M k_+ k_n \text{G51D} b m(0)^{n, \text{G51D}} t}{4(K_M + m(0))}$  using equation 4 and the following values for the various constants:  $M(t) \leq 0.4 \mu\text{M}$ ,  $m(0) = 100 \mu\text{M}$ ,  $b = 3.3 \mu\text{M}$ ,  $t = 65 \text{ h}$ . We then used this value to determine the upper bound of the relative rate of aggregation on vesicles to that of the WT protein by using equation 5.

**Derivation of the approach used to analyze highly seeded aggregation data.** For aggregation experiments at high seed concentrations ( $\mu\text{M}$ ), under which primary nucleation of  $\alpha$ -synuclein can be neglected, and under quiescent conditions, where fragmentation is negligible, the aggregation kinetics for the consumption of monomers can be described by the equation:

$$\frac{dm(t)}{dt} = -\frac{dM(t)}{dt} = -2k_+ P(t)m(t) \quad [6]$$

where  $k_+$  is the fibril elongation rate constant,  $m(t)$  the monomer concentration,  $M(t)$  is the mass concentration of fibrils and  $P(t)$  the number concentration of fibrils. At early times in the aggregation reaction, the monomer concentration and the fibril number concentration can be assumed to be constant, hence  $m(t) = m(0)$  and  $P(t) = P(0)$ , and:

$$\left.\frac{dM(t)}{dt}\right|_{t=0} = 2k_+ P(0)m(0) \quad [7]$$

By fitting a linear slope to the early time points of the aggregation reaction, we can obtain the value of  $2k_+P(0)m(0)$ . For the comparison of the rate constants of different variants, we then calculate ratios  $r$ :

$$r = \frac{\left(\frac{dM(t)}{dt}\right)_{j,i}\Big|_{t=0}}{\left(\frac{dM(t)}{dt}\right)_{i,i}\Big|_{t=0}} = \frac{2k_{+,j,i}P_i(0)m_j(0)}{2k_{+,i,i}P_i(0)m_i(0)} \quad [8]$$

$r$  is the ratio of the initial gradient fitted to the kinetic trace for monomer  $j$  elongating from fibrils of variant  $i$  ( $k_{+,j,i}$ ) and the initial gradient fitted to the kinetic trace for monomer  $i$  elongating from fibrils of variant  $i$  ( $k_{+,i,i}$ ) (i.e. homogeneous elongation).  $P_i(0)$  is the initial number concentration of fibrils from variant  $i$  and the same seed stock was used for all monomer variants.  $m_j(0)$  and  $m_i(0)$  are the initial monomer concentrations of variant  $j$  and variant  $i$ , respectively. Comparing elongation rates for monomeric proteins for the same initial monomeric protein concentration, i.e.  $m_j(0) = m_i(0)$ , elongating from fibrils of the same variant can be analyzed as:

$$r = \frac{\left(\frac{dM(t)}{dt}\right)_{j,i}\Big|_{t=0}}{\left(\frac{dM(t)}{dt}\right)_{i,i}\Big|_{t=0}} = \frac{k_{+,j,i}}{k_{+,i,i}} \quad [9]$$

**Derivation of the approach to analyze aggregation kinetics at acidic pH.** For aggregation experiments at low seed concentrations in 20 mM phosphate buffer under quiescent conditions at pH 4.8, the kinetic data can be analyzed in detail to determine the rate of amplification of  $\alpha$ -synuclein fibrils. Under these conditions both primary nucleation and fragmentation are negligible, therefore, the rate of amplification of  $\alpha$ -synuclein fibrils can be approximated to the change in the number concentration of fibrils,  $\frac{dP(t)}{dt}$ . The rate of autocatalytic amplification of  $\alpha$ -synuclein fibrils was determined at the half-time of the reaction, so that we compare these rates for the same monomer concentration  $m(t) = \frac{m(0)}{2}$ . As for the previously described analysis of elongation rate constants, we start from the linear polymerization model:

$$\frac{dm(t)}{dt} = -\frac{dM(t)}{dt} = -2k_+P(t)m(t) \quad [10]$$

To analyze  $\frac{dP(t)}{dt}$ , we have to determine the derivative of  $\frac{dM(t)}{dt}$ ,

$$\frac{d^2M(t)}{dt^2} = 2k_+ \left( \frac{dm(t)}{dt}P(t) + \frac{dP(t)}{dt}m(t) \right) \quad [11]$$

which can then be rearranged to allow the calculation of  $\frac{dP(t)}{dt}$ :

$$\frac{dP(t)}{dt} = \frac{1}{2k_+m(t)} \left( \frac{d^2M(t)}{dt^2} - 2k_+\frac{dm(t)}{dt}P(t) \right) \quad [12]$$

At the half-time  $\frac{d^2M(t)}{dt^2}$  is small for sigmoidal curves, therefore we assume that  $\frac{d^2M(t)}{dt^2} \approx 0$ , resulting in:

$$\left.\frac{dP(t)}{dt}\right|_{t=t_{1/2}} = -\frac{1}{m(t=t_{1/2})}P(t=t_{1/2})\left.\frac{dm(t)}{dt}\right|_{t=t_{1/2}} \quad [13]$$

It is defined that  $m(t = t_{1/2}) = \frac{m(0)}{2}$ .  $P(t = t_{1/2})$  can be substituted by  $-\frac{2}{m(0)k_+} \left. \frac{dm(t)}{dt} \right|_{t=t_{1/2}}$  using Eq. 10 resulting in:

$$\left. \frac{dP(t)}{dt} \right|_{t=t_{1/2}} = \left( \frac{1}{m(0)} \left. \frac{dm(t)}{dt} \right|_{t=t_{1/2}} \right)^2 \frac{4}{k_+} \quad [14]$$

$\left. \frac{dm(t)}{dt} \right|_{t=t_{1/2}}$  was determined from experimental data for WT, A30P, E46K and A53T  $\alpha$ -synuclein by taking the first derivative of the sigmoidal fits to the kinetic traces shown in Fig. 4 and used to determine  $\left. \frac{dP(t)}{dt} \right|_{t=t_{1/2}}$  for different monomer concentrations.  $\left. \frac{dP(t)}{dt} \right|_{t=t_{1/2}}$  was then normalized to the rate of the fastest aggregating monomer variant A53T:

$$r = \frac{\left( \left. \frac{dP(t)}{dt} \right|_{j,i} \right)_{t=t_{1/2}}}{\left( \left. \frac{dP(t)}{dt} \right|_{A53T,i} \right)_{t=t_{1/2}}} = \frac{\left( \frac{1}{m_{j,i}(0)} \left( \left. \frac{dm(t)}{dt} \right|_{j,i} \right)_{t=t_{1/2}} \right)^2 \frac{1}{k_{+,j,i}}}{\left( \frac{1}{m_{A53T,i}(0)} \left( \left. \frac{dm(t)}{dt} \right|_{A53T,i} \right)_{t=t_{1/2}} \right)^2 \frac{1}{k_{+,A53T,i}}} \quad [15]$$

where  $\left( \left. \frac{dP(t)}{dt} \right|_{j,i} \right)$  is the change in fibril number concentration for monomer variant  $j$  aggregating in the presence of pre-formed fibrils of variant  $i$ .  $m_{j,i}(0)$  is the initial monomer concentration of monomer variant  $j$  aggregating in the presence of pre-formed fibrils of variant  $i$ . We found that the elongation rate in the presence of pre-formed fibrils is only marginally affected by the mutations (see above), therefore  $k_{+,j,i} \approx k_{+,A53T,i}$  and since we form ratios for the same initial monomer concentration, we obtain  $m_{j,i}(0) = m_{A53T,i}(0)$ , further simplifying the analysis. Then the average of the ratios for each variant over the monomer concentrations can be defined as:

$$r = \frac{\left( \left. \frac{dP(t)}{dt} \right|_{j,i} \right)_{t=t_{1/2}}}{\left( \left. \frac{dP(t)}{dt} \right|_{A53T,i} \right)_{t=t_{1/2}}} = \left( \frac{\left( \left. \frac{dm(t)}{dt} \right|_{j,i} \right)_{t=t_{1/2}}}{\left( \left. \frac{dm(t)}{dt} \right|_{A53T,i} \right)_{t=t_{1/2}}} \right)^2 \quad [16]$$

1. Buell AK et al. (2014) Solution conditions determine the relative importance of nucleation and growth processes in  $\alpha$ -synuclein aggregation. *Proc. Natl. Acad. Sci. U.S.A.* 111(21):7671–7676.
2. Galvagnion C et al. (2015) Lipid vesicles trigger  $\alpha$ -synuclein aggregation by stimulating primary nucleation. *Nat. Chem. Biol.* 11(3):229–234.
3. Hoyer W et al. (2002) Dependence of alpha-synuclein aggregate morphology on solution conditions. *J. Mol. Biol.* 322(2):383–393.
4. Meisl G et al. (2016) Molecular mechanisms of protein aggregation from global fitting of kinetic models. *Nat Protoc* 11(2):252–272.

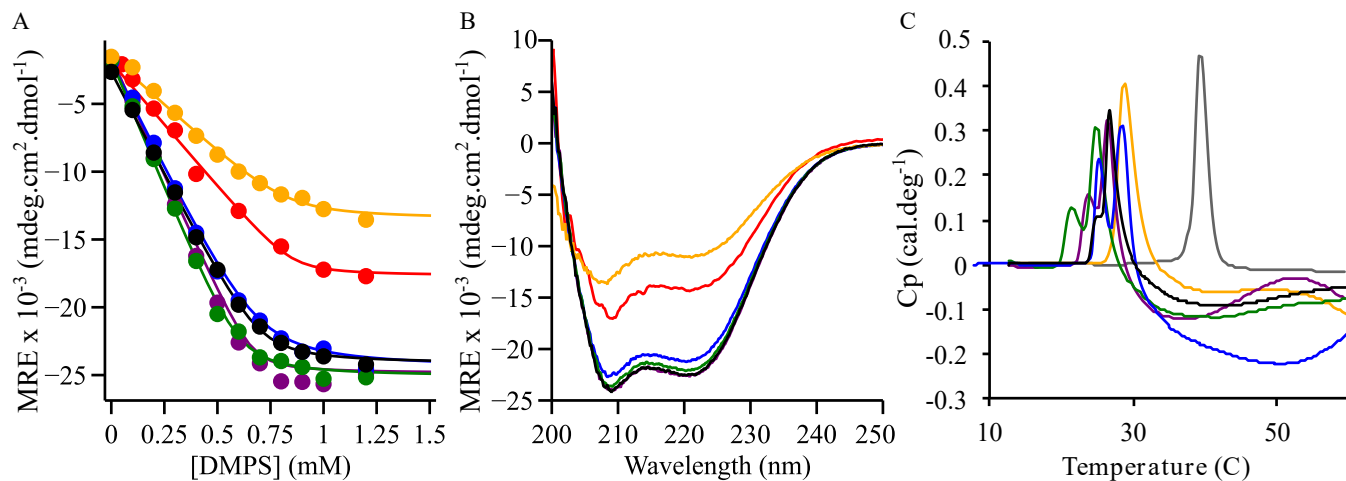


**Fig. S1.** Binding of WT and disease-associated variants of  $\alpha$ -synuclein to DMPS vesicles. Change in the Mean Residue Ellipticity measured at 222 nm (A) and CD spectra (B) of  $\alpha$ -synuclein (WT (black), A30P (yellow), E46K (green), H50Q (blue), G51D (red), A53T (purple)) measured at pH 6.5 and 30°C. The binding curves were fitted to a 1-step binding model (see Methods for details) and led to dissociation constants ( $K_D$ ) of  $0.38 \pm 0.13$  (WT),  $0.55 \pm 0.37$  (A30P),  $0.34 \pm 0.20$  (E46K),  $0.61 \pm 0.27$  (H50Q),  $0.16 \pm 0.35$  (G51D) and  $0.18 \pm 0.14$  (A53T)  $\mu$ M and stoichiometries ( $L$ ) of  $28.2 \pm 0.8$  (WT),  $33.2 \pm 3.4$  (A30P),  $30.4 \pm 1.6$  (E46K),  $35.2 \pm 2.1$  (H50Q),  $42.5 \pm 4.5$  (G51D) and  $26.7 \pm 1.1$  (A53T). (C) DSC traces of DMPS vesicles in the absence (grey) or the presence of WT (black), A30P (yellow), A53T (purple), E46K (green) or H50Q (blue)  $\alpha$ -synuclein at pH 6.5.

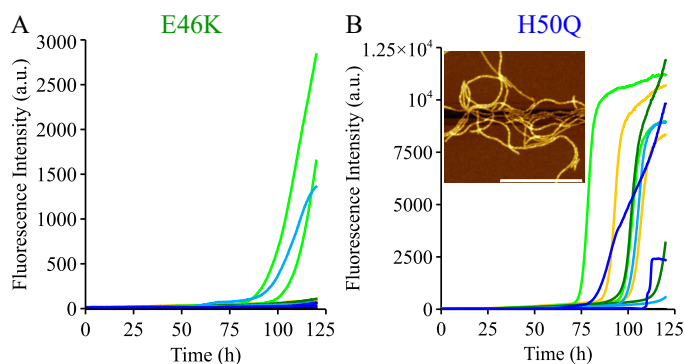


**Fig. S2.** DMPS induced aggregation of E46K and H50Q. (A,B) Change in ThT fluorescence intensity when  $\alpha$ -synuclein (E46K (A), H50Q (B)) was incubated in the absence (black) and in the presence of 100  $\mu$ M DMPS under quiescent conditions at pH 6.5 and 30°C. The protein concentrations used in this study were: 20 (dark blue), 40 (light blue), 60 (green), 80 (light green) and 100  $\mu$ M (yellow). The inset of the panel B shows the AFM image of the fibrils formed under these conditions. The scale bar represents 1  $\mu$ m.

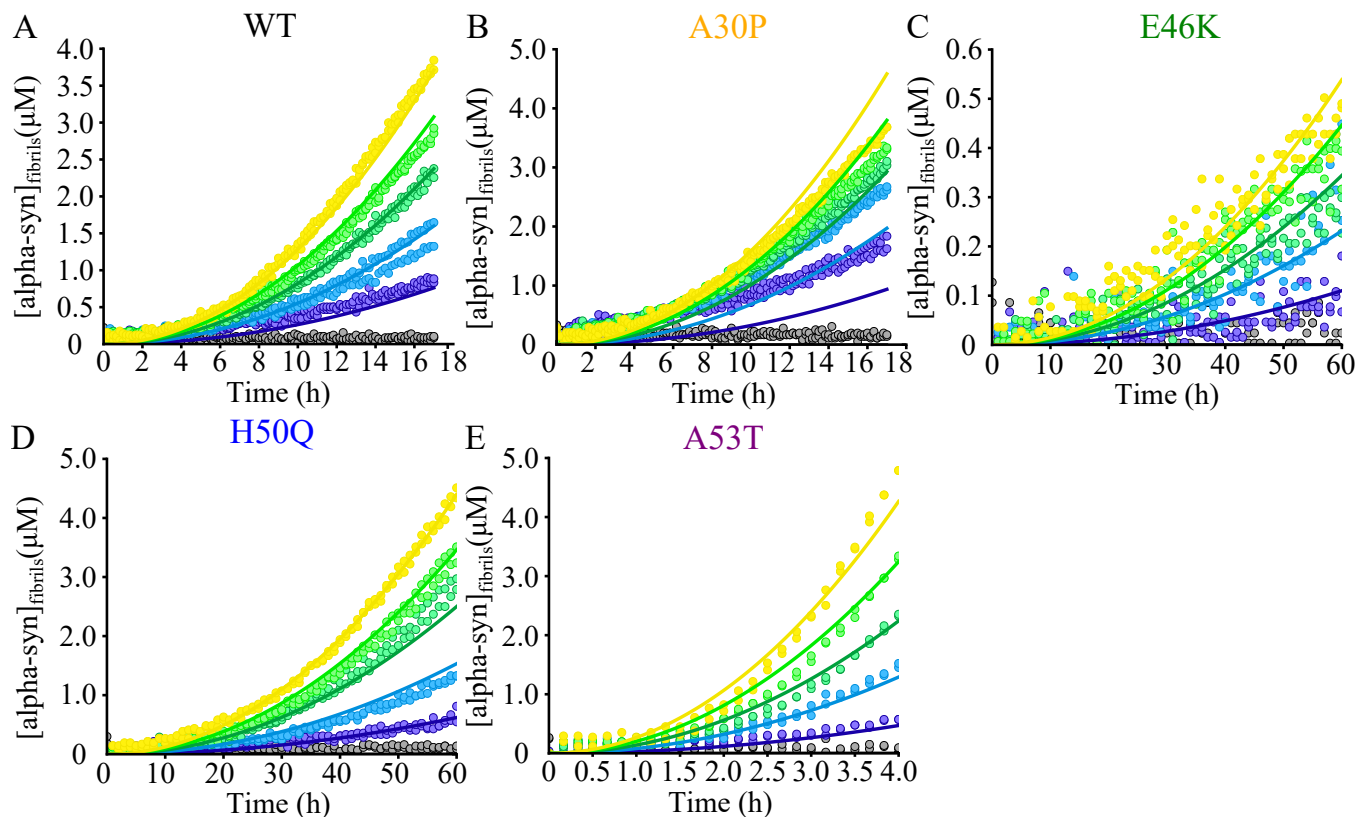


**Fig. S3.** Global analysis of WT and disease-associated variants of  $\alpha$ -synuclein using a one-step nucleation model. Change in ThT fluorescence intensity when  $\alpha$ -synuclein (WT (A), A30P (B), E46K (C), H50Q (D), A53T (E)) was incubated in the absence (black) and in the presence of 100  $\mu$ M DMPS under quiescent conditions at pH 6.5 and 30°C. The protein concentrations used in this study were: 20 (dark blue), 40 (light blue), 60 (green), 80 (light green) and 100  $\mu$ M (yellow). Global fitting of the early times of the aggregation curves to a one-step nucleation model leads to the determination of the product  $k_n k_+ (1.2 \pm 0.6 \cdot 10^{-4}$  (WT),  $1.47 \pm 0.03 \cdot 10^{-4}$  (A30P),  $8.8 \pm 4 \cdot 10^{-7}$  (E46K),  $9.3 \pm 1.8 \cdot 10^{-5}$  (H50Q),  $8.3 \pm 0.3 \cdot 10^{-3}$  (A53T)  $M^{-(n+1)} s^{-2}$ , and  $n (0.26 \pm 0.12$  (WT), 0.26 (A30P),  $0.22 \pm 0.10$  (E46K),  $0.49 \pm 0.04$  (H50Q),  $0.64 \pm 0.01$  (A53T)).  $K_M$  was fixed at 125  $\mu$ M. The mean squared errors were:  $1.1 \cdot 10^{-14}$  (WT),  $1.9 \cdot 10^{-13}$  (A30P),  $1.7 \cdot 10^{-15}$  (E46K),  $1.3 \cdot 10^{-14}$  (H50Q),  $1.3 \cdot 10^{-14}$  (A53T)  $\mu M^2$ .



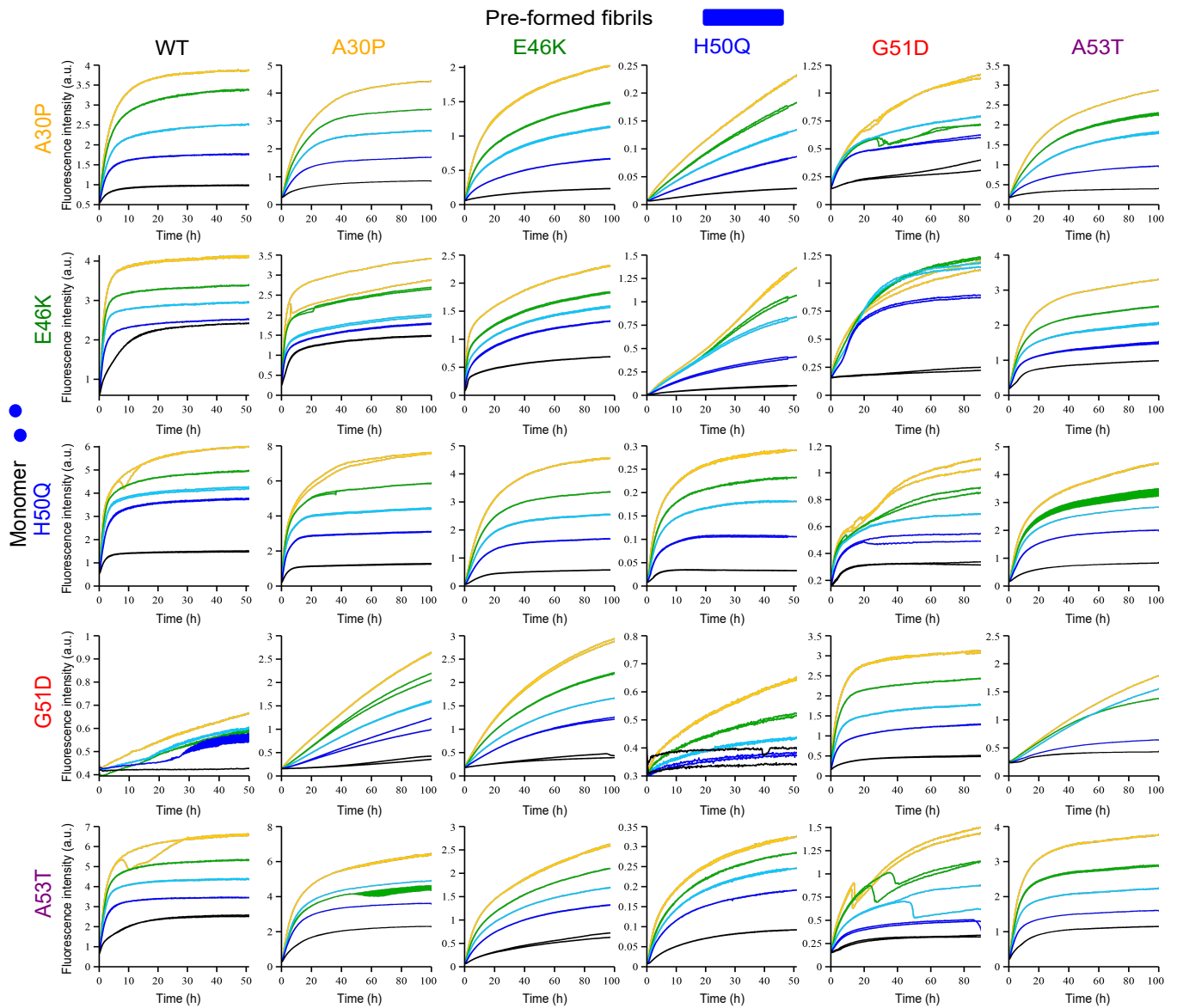


**Fig. S4.** Fibril elongation of WT  $\alpha$ -synuclein and its disease-associated variants. Change in ThT fluorescence when monomeric  $\alpha$ -synuclein at different concentrations (10 (black), 30 (blue), 50 (light blue), 70 (green) and 100 (yellow)  $\mu$ M) was incubated in the presence of 5  $\mu$ M pre-formed fibrils from the indicated mutational variant (A30P, E46K, H50Q, G51D and A53T) under quiescent conditions at pH 6.5 and 37°C.

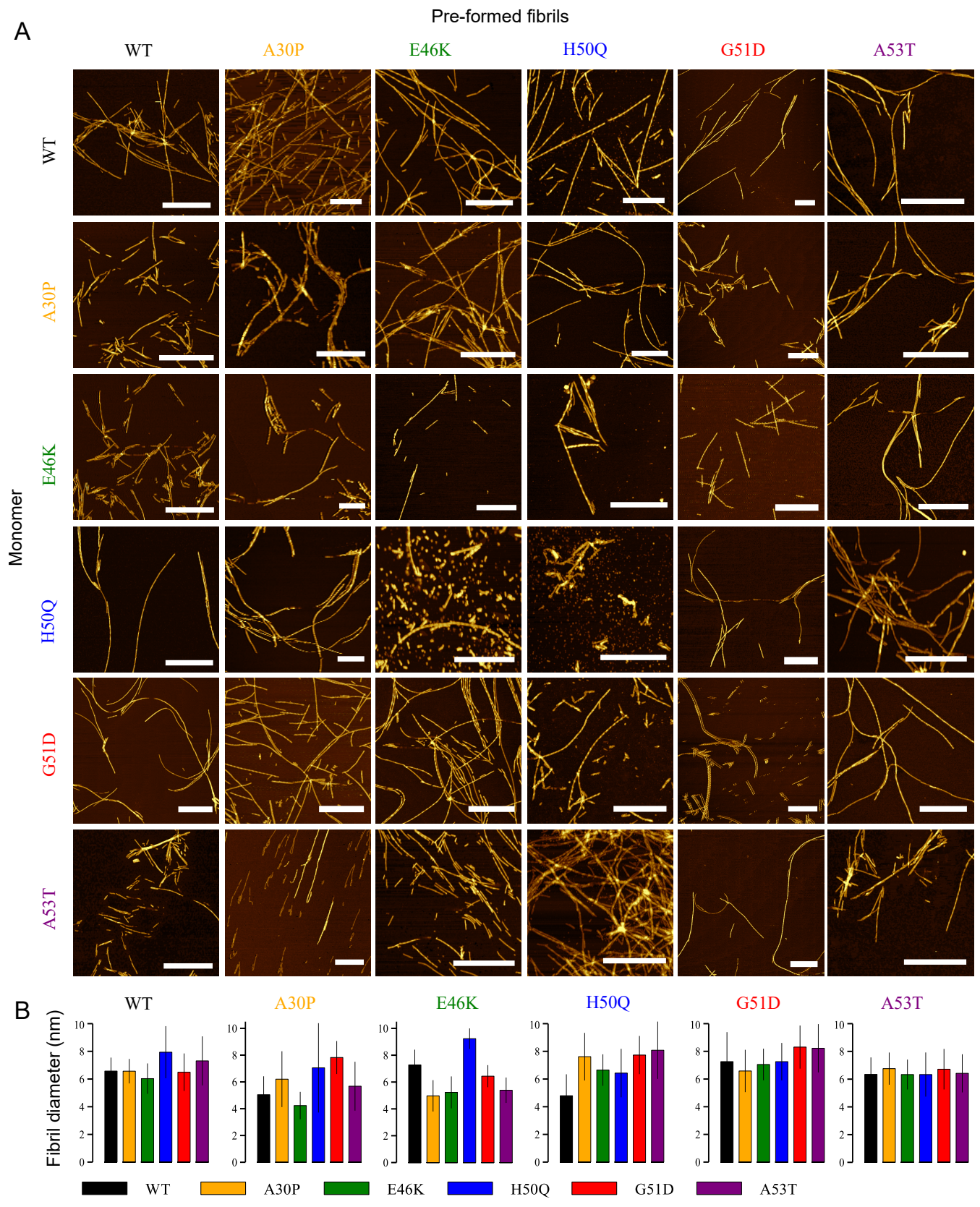


**Fig. S5.** Fibril morphology of  $\alpha$ -synuclein WT and its disease associated mutant variants. (A) AFM images of the fibrils formed by  $\alpha$ -synuclein and its disease-associated variants for each monomeric variant aggregating in the presence of pre-formed fibrils from each variant. The scale bars represent 1  $\mu$ m. (B) Average diameter of the fibrils.

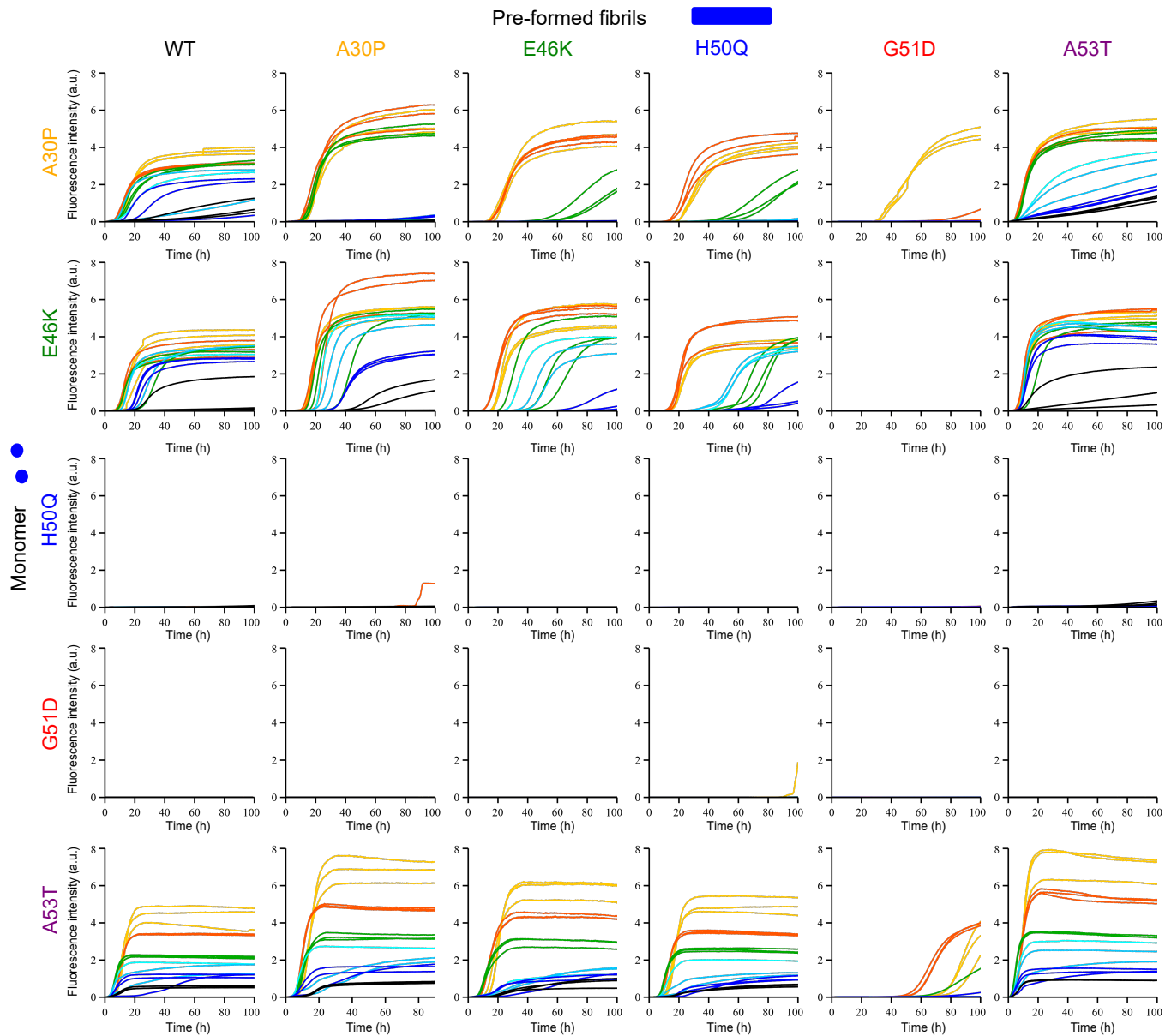


**Fig. S6.** Fibril amplification at mildly acidic pH of WT  $\alpha$ -synuclein and its disease-associated variants. Change in ThT fluorescence intensity when monomeric  $\alpha$ -synuclein (WT, A30P, E46K, H50Q, G51D and A53T) was incubated in the presence of 35 nM pre-formed fibrils of the indicated variant (A30P, E46K, H50Q, G51D and A53T) under quiescent conditions at pH 4.8 and 37°C. The protein concentration used in this study were: 20 (black), 30 (dark blue), 40 (light blue), 50 (green), 70 (light green) and 100  $\mu$ M (yellow).

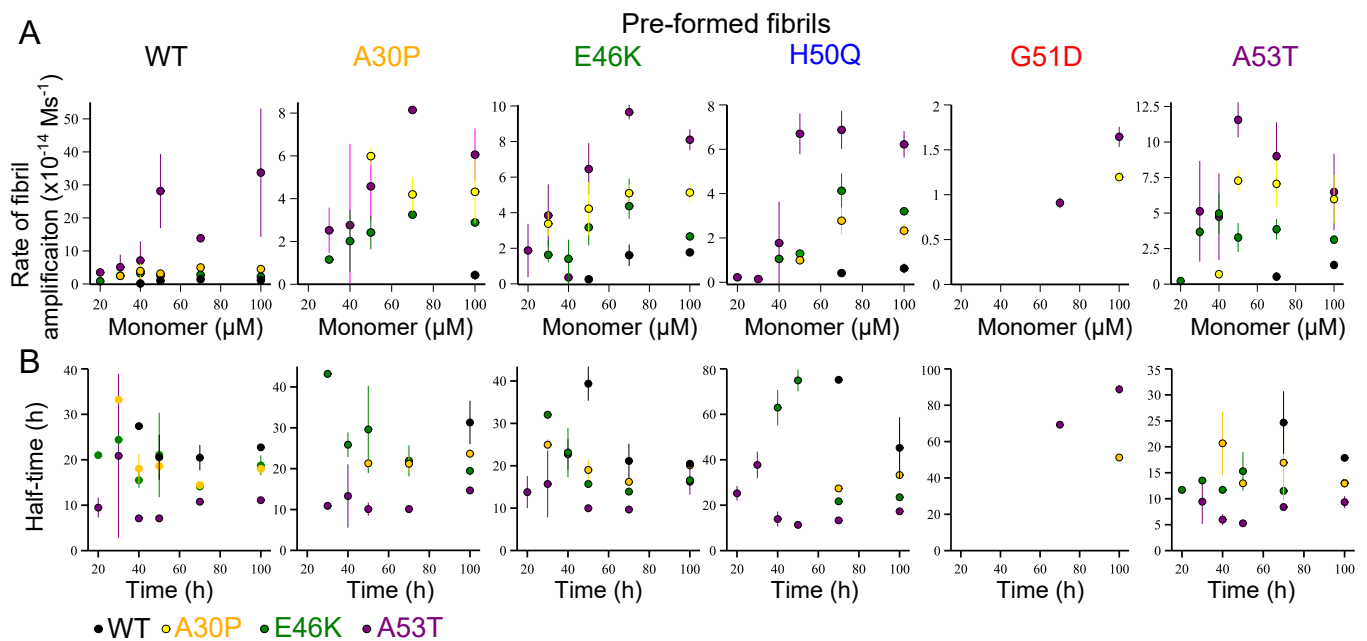


**Fig. S7.** Fibril amplification at mildly acidic pH of WT  $\alpha$ -synuclein and its disease-associated variants. (A) Variation of the rate of fibril amplification of WT (black), A30P (orange), E46K (green), H50Q (blue), G51D (red) and A53T (purple) from WT, A30P, E46K, H50Q, G51D and A53T seeds, respectively, with increasing concentrations of monomeric protein. (B) Half-times of the aggregation experiments.

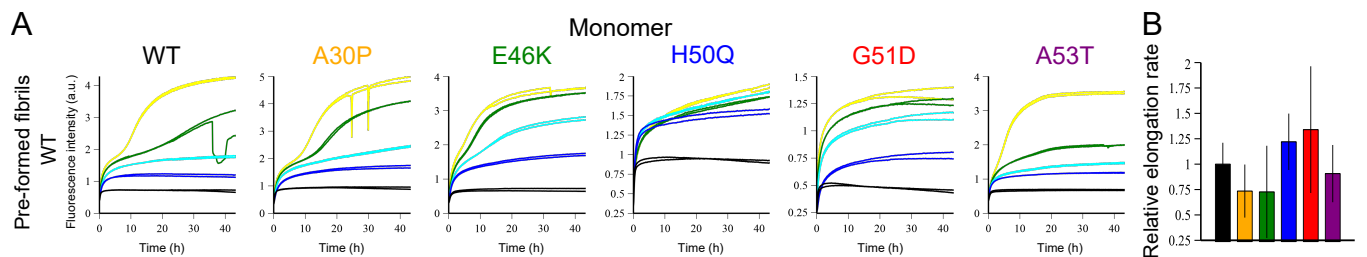


**Fig. S8.** The elongation rate of  $\alpha$ -synuclein is only mildly affected by the disease-associated mutations at acidic pH. (A) Change in ThT fluorescence when monomeric  $\alpha$ -synuclein of the indicated mutational variant (WT, A30P, E46K, H50Q, G51D and A53T) at different concentrations (10 (black), 30 (blue), 50 (light blue), 70 (green) and 100 (yellow)  $\mu\text{M}$ ) was incubated in the presence of 5  $\mu\text{M}$  pre-formed fibrils of the WT protein under quiescent conditions at pH 4.8 and 37 $^{\circ}\text{C}$ . (B) Normalized ratios of the elongation rates of the disease-associated variants relative to the rate of the WT protein.

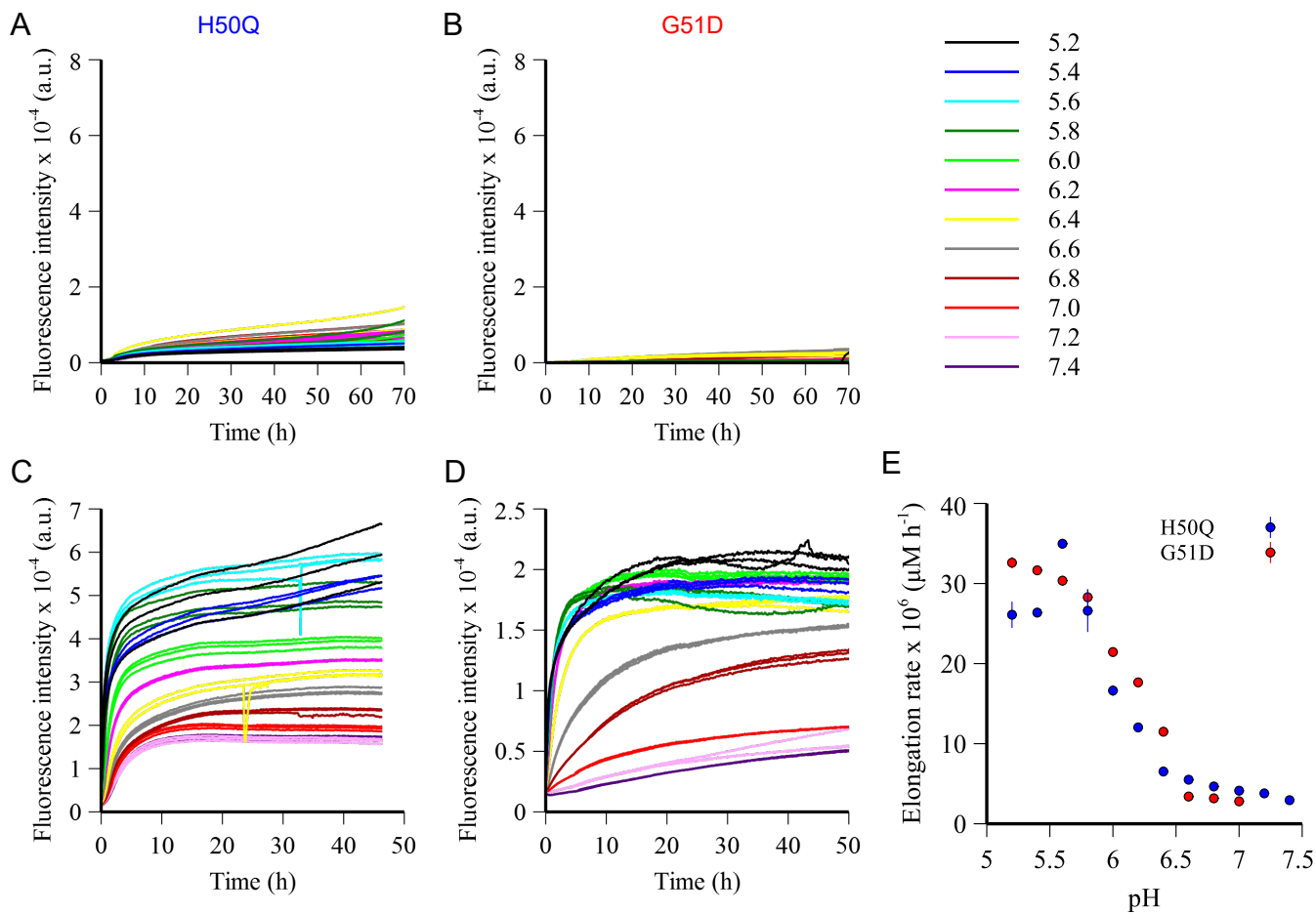


**Fig. S9.** The pH dependence of fibril amplification and elongation of H50Q and G51D  $\alpha$ -synuclein. Change in ThT fluorescence when monomeric H50Q (A) or G51D (B)  $\alpha$ -synuclein ( $50 \mu\text{M}$ ) was incubated in the presence of  $35 \text{ nM}$  preformed H50Q or G51D seed fibrils, respectively, under quiescent conditions at the pH values indicated and  $37^\circ\text{C}$ . Change in ThT fluorescence when monomeric H50Q (C) or G51D (D)  $\alpha$ -synuclein ( $50 \mu\text{M}$ ) was incubated in the presence of  $5 \mu\text{M}$  pre-formed H50Q (C) or G51D (D) seed fibrils under quiescent conditions at the pH values indicated and  $37^\circ\text{C}$ . (E) pH dependence of the elongation rate of H50Q (blue) and G51D (red). Rates were determined as described.

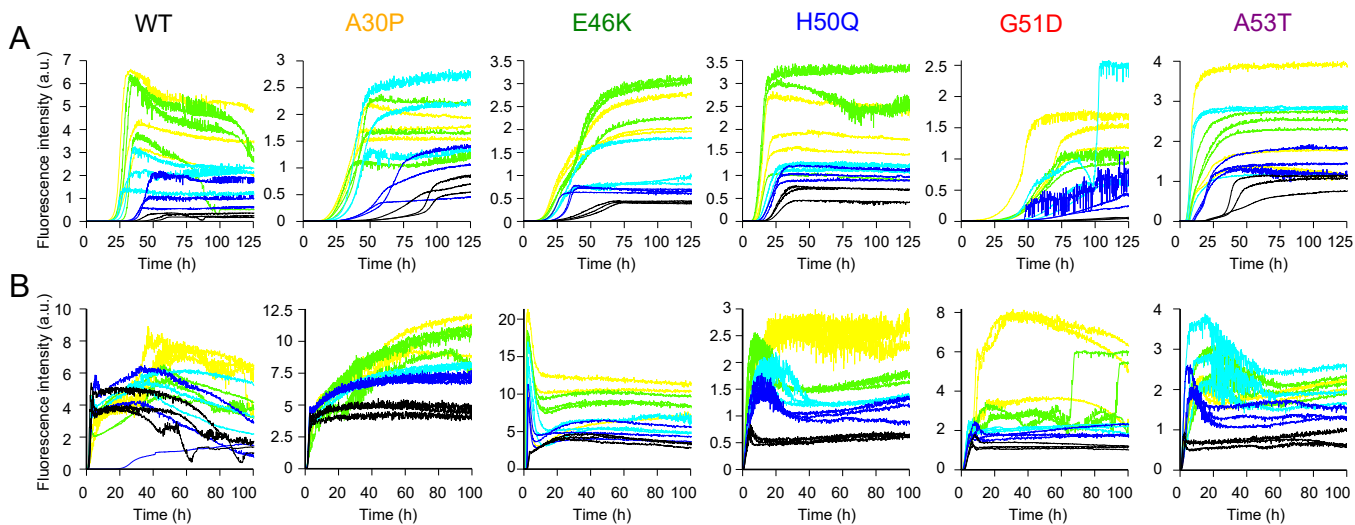


**Fig. S10.** Aggregation under shaking conditions. Aggregation of WT  $\alpha$ -synuclein and its disease associated mutant variants (A30P, E46K, H50Q, G51D, A53T) under shaking conditions at pH 6.5 (A) or pH 4.8 (B), respectively ( $37^\circ\text{C}$  and  $1100 \text{ rpm}$ ). The ThT fluorescence was measured in aggregation experiments with different monomer concentrations (black:  $20 \mu\text{M}$ , blue:  $40 \mu\text{M}$ , cyan:  $60 \mu\text{M}$ , green:  $80 \mu\text{M}$ , yellow:  $100 \mu\text{M}$ ).

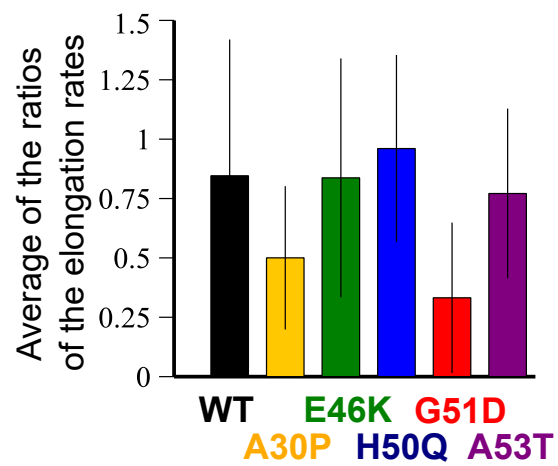


**Fig. S11.** Mutations associated with Familial Parkinson's disease only mildly affect the elongation step of  $\alpha$ -synuclein aggregation. Average of the ratios of elongation rates determined for the elongation of monomeric variants from pre-formed fibrils from all  $\alpha$ -synuclein variants studied in this work (data from Fig. 3B).